Optimizing Electric Vehicle Charging Stations and Distributed Generators in Smart Grids: A Multi-Objective Meta-Heuristic Approach

Divya Bharathi Raj, *Member, IEEE*, and Venkatakirthiga Murali, *Member, IEEE*

***Abstract*—The global transition towards electric mobility has significantly increased the demand for efficient and consumer-friendly Electric Vehicle Charging Stations (EVCSs). As electric vehicles (EVs) continue to penetrate transportation systems, optimal integration of EVCSs within power distribution infrastructure becomes critical, not only to ensure seamless user experience but also to maintain the reliability and efficiency of electrical networks. Traditionally, EVCS planning has been carried out solely within the context of Radial Distribution Networks (RDNs), neglecting key consumer-centric factors such as travel comfort and accessibility within the road network (RN). This paper proposes a novel, consumer-aware methodology for optimally placing EVCSs and Distributed Generators (DGs) in a combined RDN-RN framework. The objective is to minimize active power loss, voltage variation, and EV consumer cost, measured through two proposed indices, while accounting for realistic travel behavior and preferences. The proposed approach utilizes a Modified Weighted Teaching Learning Based - Particle Swarm Optimization Algorithm (MWTLB-PSA) and proceeds in three stages: EVCS site selection based on road network considerations, DG placement using predetermined EVCS locations, and a final stage of simultaneous optimization of both elements. To validate the approach, a standard IEEE 33-bus RDN integrated with a 25-node RN is employed as the test system. Results demonstrate that the joint optimization of DGs and EVCSs via the proposed method significantly enhances network performance and consumer convenience. Notably, the solution achieves a reduced active power loss of 57.75 kW and an EVCCI value of 0.3958, indicating a substantial improvement over existing hybrid TLBO and PSO-based techniques. Furthermore, the proposed method leads to installation cost savings ranging from 2.51% to 18.21% compared to earlier strategies, underscoring its practical value in smart grid planning and deployment.**

Link to graphical and video abstracts, and to code:
https://latamt.ieeer9.org/index.php/transactions/article/view/9630

***Index Terms*—Distributed energy resources; Electric vehicle charging stations; Energy management; Electric vehicle; Metaheuristic algorithms; Multi-objective optimization; Power distribution systems;Smart grid planning.**

I. Introduction

EVS have emerged as a viable and sustainable alternative to fossil fuel-based vehicular technologies in recent years [1]. Many nations, especially those with resource constraints, view EV adoption as a strategic solution to address fossil fuel dependency and reduce carbon dioxide emissions [2,3]. Many Governments have implemented various strategies to encourage the adoption of EVs, aiming to mitigate petroleum usage and environmental degradation. Zero-emission vehicles are critical in reducing carbon footprints, complemented by increased use of renewable energy sources (RES) and advanced control mechanisms [4-6]. However, the widespread adoption of EVs also poses challenges to future power systems, such as voltage variations, system losses, and line stress, which necessitate effective mitigation strategies [7]. Ensuring the resilience of power systems against such technical challenges is essential, emphasizing the need for efficient planning and optimization of EVCSs [8]. Managing these challenges becomes essential for a seamless and long-lasting shift towards broad EV adoption worldwide as the EV industry develops.

The appropriate siting and sizing of EVCSs have gained significant attention in recent years due to the growing penetration of EVs in transportation and power systems. In this regard, many researchers have worked towards EVCS infrastructure planning, where Deb et al. [9] design an EV charging infrastructure plan for Guwahati, India, using a hybrid optimization approach that balances economic, grid, and user-centric factors. Pareto-optimal solutions were obtained through a combination of chicken swarm and teaching-learning-based algorithms (CSO-TLBO), refined by fuzzy decision-making. Zhu et al. [10] determine optimal positioning of EVCSs as a maximum flow coverage problem, using genetic algorithms (GA), expanded P-centre techniques for effective solutions. Advanced planning methodologies proposed by W. Yao et al. [11] include multi-objective optimization, focusing on minimizing construction and operational costs while optimizing traffic flow and RDN performance. Rawa et al. [12] and Clairand et al. [13] explore the techno-economic and ecological implications of EVCS deployment, integrating environmental factors, installation costs, and driver-specific demands. D.B.R et al. [14] and A. Pal et al. [15] have investigated Vehicle-to-Grid (V2G) capabilities that have further enhanced this integration, contributing to grid stability and resilience. Further, the optimal placement of DGs is crucial for minimizing power losses in RDNs. Many studies have dealt with the optimal planning of DGs, including financial intricacies, enhancements to power quality, and adherence to voltage and current harmonic requirements. Babu et al. [16] have explored the Harris Hawk Optimization algorithm (HHO)

The associate editor coordinating the review of this manuscript and approving it for publication was Gabriel Pinto (*Corresponding author: Venkatakirthiga Murali*).

D. B. Raj, and Venkatakirthiga Murali, are with the Department of Electrical and Electronics Engineering, National Institute of Technology Tiruchirappalli, Tamilnadu, India (e-mails: 407121005@nitt.edu, and mvkirthiga@nitt.edu).

to strategically integrate DGs in RDN. This method enhances voltage stability, minimizes power losses, and boosts system performance, showcasing superior efficiency over conventional techniques. Lakshmi et al. [17] have adopted a hybrid genetic dragonfly algorithm (GA-DF) to determine the best DG locations and sizes, in standard IEEE test systems to reduce active power losses (APL). Prasad et al. [18] have used the Elephant Herding Optimization (EHO) algorithm to optimize DG sizing, which shows improved results by incorporating with type III DG units at 0.9 power factor. Memarzadeh et al. [19] have proposed an analytical index to optimize DG placement and sizing by considering loss sensitivity, voltage stability, and reliability factors. Kumar et al. [20] have suggested methods for optimizing DG placement and sizing, focusing on reduced losses, improved voltage profiles, and enhanced system reliability. It covers traditional, AI, hybrid, and software-based approaches, offering insights for researchers. Haider et al. [21] have proposed optimizing the placement and sizing of DG units in RDN, leveraging a multi-objective particle swarm optimization (PSO) algorithm to reduce power loss, improve voltage profiles, and enhance system reliability. Selim et al. [22] have proposed a hybrid optimization method using analytical techniques and the sine-cosine algorithm (AT-SCO) for efficient DG placement in RDN. Zabihia et al. [23] have highlighted the relevance of RES and PHEVs in the establishment of smart grids by examining their effects on power networks through load flow (LF), short-circuit analysis (SCA), and economic assessment using DIgSILENT. With an emphasis on decentralized energy trade, smart grid emancipation, and upcoming possibilities for cleaner energy transformations, along with advancements like DSM and battery management, Zabihia et al. [24,25] have investigated blockchain-enabled EV charging infrastructure. A hybrid GA-PSO strategy, verified by a thorough sensitivity analysis, is presented by B.V. Kumar et al. [26] for the best placement of EVCS and capacitors in RDN, reducing losses, improving V2G interaction, and optimizing net revenue.

Subsequently, researchers have focused on combining EVCS and DG units in RDN to improve the system's reliability and efficiency. Ponnam et al. [27] have explored the integration of DG into the RDN as a potential solution to mitigate the negative impacts of EVCS deployment, such as increased losses and voltage instability. Ahmad et al. [28] have proposed that the simultaneous planning of DG units and EVCS in RDN is a key area of research to address the compounded challenges of EV adoption. This approach has aimed at optimizing network features such as power losses, voltage profiles, and system reliability while considering traffic flow and land costs for EVCS placement. Bilal et al. [29] have explored RES-powered hybrid systems for EV charging in India, optimizing cost and reliability using a modified salp-swarm algorithm (SSA). The findings highlight the potential to reduce grid dependency and support sustainable EV infrastructure in developing nations. Chakraborty et al. [30] have focussed on aligning EVCS deployment with DG capabilities to ensure long-term sustainability and efficiency in power systems using advanced models and algorithms. Hariri et al. [31] have introduced a new hierarchical optimization method that concurrently allocates protective devices, DGs, and EVCS to improve power system reliability. Vijay et al. [32] have presented a multi-objective approach for planning EVCS and DG, optimizing power loss, voltage stability, and user costs using the Rao-3 algorithm on an integrated power and RN. Asghari Rad et al. [33] have proposed a model for the ideal placement, size, and timing of EV parking lots to maximize owner profitability and meet Plug-in hybrid EV (PHEV) parking demand while taking into account urban spatial constraints and RDN restrictions using GA-Mixed linear integer programming (GA-MILP). Applying Multi-objective GWO (MOGWO) and fuzzy decision-making techniques, Shukla et al. [34] have created a multi-objective planning model for fast EVCS (FEVCS), maximizing the performance of RDN and EV service while taking waiting time and service radius into account. Skaloumpakas et al. [35] have proposed a logical multi-criteria decision strategy (MCDS) for strategically placing EVCS on highways to encourage economic investment decisions. It addresses range anxiety by considering factors including traffic intensity, accessibility to important places, and EV driving range limits. Amini et al. [36] have employed GA and PSO optimization techniques for the joint deployment of EV parking spaces and RES, balancing technological limitations and economic advantages while minimizing system losses. A detailed overview and comparison on key research contributions towards the Placement of DG and EVCS have been presented in Table 1.

Studies from Refs. [9-15] explore the strategic placement of EVCSs in RDNs using metaheuristic optimization techniques, focusing on minimizing power loss and improving voltage stability. Refs. [16–22] extend this work by incorporating DG units, emphasizing power loss reduction and voltage enhancement. Refs. [23, 26-31,36] provide a simultaneous allocation of EVCSs and DGs or RES for the better performance improvement of RDNs. Ref [35] deals with the placement of EVCS on highways, considering RN constraints. Refs. [32-34] investigate the simultaneous placement of EVCS and DG units, aiming to reduce APL and improve voltage stability in coupled RDN and RN. Despite these research contributions and advancements, none of the earlier studies have directly addressed the consumer costs associated with EVs, an important aspect that has yet to be adequately explored. Hence, the authors of this paper have extensively focused on incorporating the consumer cost as well as the customer preference, besides focusing on technical performance improvement. The workflow explaining the proposed work adopted in this paper is displayed in Fig. 1.

The integration of EVCS into the RDN has been extensively explored in recent studies. Most researchers have primarily viewed EVCS as electrical loads, with their placement guided by economic benefits. However, only a limited number of studies have addressed the simultaneous optimization of EVCS placement and sizing while evaluating their effects on RDN. These studies highlight how improper EVCS integration could lead to increased network losses and significant voltage deviations. To encounter these effects, many investigations have focused on incorporating capacitors, DGs, and RES, aiming to mitigate the adverse impacts of EVCS by enhancing voltage

TABLE I
COMPARISON OF OPTIMIZATION TECHNIQUES FOR EVCS AND DG/RES INTEGRATION

Ref No	Year	EVCS	DG/RES	Power Loss	Voltage Stability	EVCCI	Optimization Techniques
9	2016	✓	✗	✓	✓	✗	CSO-TLBO
10	2016	✓	✗	✓	✓	✗	GA
11	2014	✓	✗	✓	✓	✗	MOEA/D
12	2021	✓	✗	✓	✓	✗	IGWO
13	2020	✓	✗	✓	✓	✗	NMA
14	2022	✓	✗	✓	✓	✗	HTLBO-PSO
15	2023	✓	✗	✓	✓	✗	GWO, WO
16	2022	✗	✓	✓	✓	✗	HHO, TLBO
17	2021	✗	✓	✓	✓	✗	GA-DF
18	2019	✗	✓	✓	✓	✗	EHO
19	2020	✗	✓	✓	✓	✗	Index based
20	2023	✗	✓	✓	✓	✗	AI, hybrid
21	2021	✗	✓	✓	✓	✗	PSO
22	2021	✗	✓	✓	✓	✗	AT-SCO
23	2024	✓	✓	✓	✓	✗	LF, SCA
26	2025	✓	✓	✓	✓	✗	GA-PSO
27	2020	✓	✓	✓	✓	✗	HHO, TLBO
28	2022	✓	✓	✓	✓	✗	GA
29	2023	✓	✓	✓	✓	✗	SSA
30	2022	✓	✓	✓	✓	✗	SOS
31	2019	✓	✓	✓	✓	✗	Hybrid GA-PSO
32	2023	✓	✓	✓	✓	✓	PSO, JA, RAO 3
33	2024	✓	✓	✓	✓	✗	GA-MILP
34	2019	✓	✓	✓	✓	✗	MOGWO
35	2022	✓	✗	✗	✗	✗	MCDS
36	2017	✓	✓	✓	✓	✗	GA, PSO
This work		✓	✓	✓	✓	✓	MWTLB-PSA

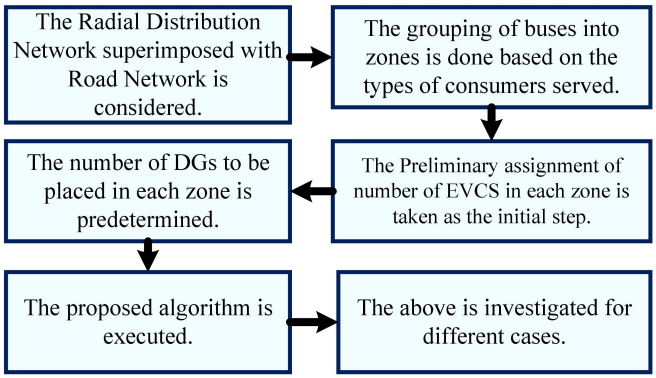

Fig. 1. Workflow of the proposed EVCS and DG planning strategy integrating RDN and RN.

stability and reducing power losses. Despite this focus, most of the research remains network-centric, often overlooking consumer preferences such as minimal travel time and distance to charging stations. Additionally, the studies in [37] review the planning of EVCS in a coupled RDN and RN. The main shortcomings identified in [37] are explicitly addressed in this work through several methodological improvements.

- First, the proposed study introduces an integrated modeling framework that combines road networks with radial distribution networks, directly addressing the absence of coupling between power and transportation systems in prior research.
- Second, a spatially resolved modeling approach is adopted rather than average-based assumptions, incorporating consumer charging behavior as a function of driving distance. This allows for more geographically accurate and future-oriented grid planning.
- Third, although the current implementation focuses on conventional charging stations, the existing model structure is readily extensible to accommodate different charger types—such as slow and fast chargers—by parameterizing load and cost inputs within the existing constraint framework.
- Finally, the switch from strictly theoretical models is signalled by the employment of an IEEE 33-bus RDN combined with a 25-node RN, offering a semi-realistic case study that forms the basis for extensive applications in real life.

Addressing these challenges is crucial for the effective deployment of EVCS in modern transportation and power systems. The following summary gives the primary contributions of the work.

1) The model incorporates the proximity of demand points to EVCS, ensuring reduced energy loss and minimal travel distance for users.
2) The proposed methodology integrates DG units with EVCSs to mitigate increased losses and degraded volt-

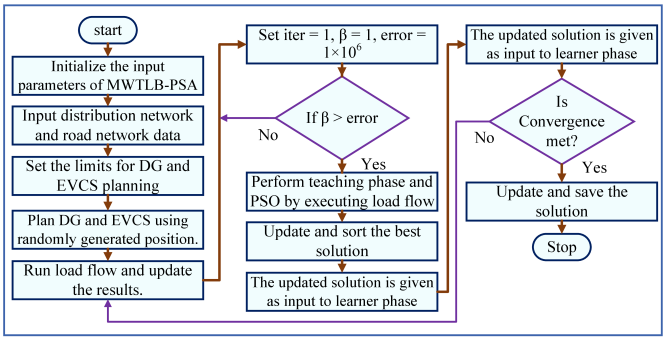

Fig. 2. Detailed flowchart of the proposed hybrid MWTLB-PSA optimization methodology.

age profiles, improving network performance.

3) The Modified Weighted Teaching Learning-Based Particle Swarm Algorithm (MWTLB-PSA) is proposed to achieve optimal placement and sizing of EVCS and DG units, balancing network and consumer needs.
4) The study presents an elementary model for EVCS and DG optimization, emphasizing the EV user's preference for the nearest charging station with minimal energy loss.

This contribution ensures a balanced approach that addresses technical and consumer-related aspects of EVCS and integration. The remaining part of the paper is organized as follows: Section II explains the formulation of the objective function. The proposed algorithm is elaborated in Section III. Section IV gives a detailed discussion of the results. Conclusions and future scope are presented in Section V.

II. Proposed Methodology

The proposed work has attempted to arrange EVCSs and DG units best while minimizing active power loss and EV consumer costs. The workflow adopted is shown already in Fig.1. Since this procedure involves the simultaneous identification of optimal location and sizing of DG units and EVCS units, a robust objective function (minimization function) with essential constraints needs to be formulated. Also, robust and effective optimization techniques are required to execute the proposed workflow to arrive at the optimal location and sizing of the DG units and EVCS units concurrently. Hence, the Hybrid TLBO-PSO algorithm is adopted, and the investigations are done with the standard 33-bus distribution system superimposed with the 25-bus RN, as explained in sections III and IV. The proposed methodology is depicted in Fig.2 as follows.

A. Multi Objective Function

The proposed work attempts to optimally place EVCS and DG units while minimizing both active power loss and EV consumer costs.

1) EV Consumer Cost Index (EVCCI): The ability of an EV user to choose the closest Charging Station (CS) eliminates the energy loss associated with traveling to distant CSs. Considering **P** potential CS locations and **m** charging demand nodes (part of the road network), the planning procedure starts by calculating the distance from each **mth** demand node to all available CSs. These distances are stored in the distance matrix **D** of order **[m, z]**, where **z** $\in$ **P**, as follows:

$$D = \begin{bmatrix} d_{1c_1} & \cdots & d_{1c_z} \\ \vdots & \ddots & \vdots \\ d_{mc_1} & \cdots & d_{mc_z} \end{bmatrix}, \tag{1}$$

where d_{ic_j} is the distance from demand node i to candidate CS location j.

After comparing distances from each demand node to all CSs, EVs at a given node are assigned to the closest CS. These minimum distances are stored in the matrix **DD** of order **[m, 1]**, given by

$$DD = \begin{bmatrix} \min(d_{1c_1}, \ldots, d_{1c_z}) \\ \vdots \\ \min(d_{mc_1}, \ldots, d_{mc_z}) \end{bmatrix}. \tag{2}$$

The sequence of demand points is denoted by $d = d_1, d_2, \ldots, d_m$, while the number of charging nodes from the road network is denoted by $c = c_1, c_2, \ldots, c_p$. The EV consumer cost is computed using

$$\text{EV}_{\text{consumer cost}} = \sum_{t=1}^{m} DD(n) \cdot N_{\text{EV}}(n) \cdot EC_{\text{EV}} \cdot \lambda_E, \tag{3}$$

where EC_{EV} is the energy consumption per EV, λ_E is the electricity price, and $N_{\text{EV}}(n)$ is the number of EVs at node n.

The maximum distance that an EV consumer has to travel from the m^{th} demand node is obtained by evaluating all distances from that node to the **p** charging nodes and selecting the greatest value. These maximum values form the matrix $\mathbf{DD}_{\text{max}}$. The maximum EV consumer cost is then computed as

$$\text{EV}^{\text{max}}_{\text{consumer cost}} = \sum_{t=1}^{m} \left[DD_{\text{max}}(n) \cdot N_{\text{EV}}(n) \cdot EC_{\text{EV}} \cdot P_E \right], \tag{4}$$

where P_E is the per-unit cost associated with long-distance EV travel.

Finally, the EV Consumer Cost Index (EVCCI) is defined as

$$\text{EVCCI} = \frac{\text{EV}_{\text{consumer cost}}}{\text{EV}^{\text{max}}_{\text{consumer cost}}}. \tag{5}$$

2) Active Power Loss Index (APLI): CSs are often regarded as the load at the substation for power distribution. When CS is added to RDN, the system is subject to increased tension, which affects bus voltage magnitude and power losses. Furthermore, misplacing CS results in unusually high losses and changes the healthy voltage profile. This impact is mitigated by adding DG units. Hence, APLI indicates the change in base APL concerning losses due to EVCS and DG units. Mathematically, the APLI is calculated as

$$\text{APLI} = 1 - \frac{\text{APL}_{\text{base}}}{\text{APL}_{\text{EVCS/DG}}}, \tag{6}$$

where APL_{base} and $\text{APL}_{\text{EVCS/DG}}$ represent the active power loss under base conditions and after integrating EVCS or DG units, respectively.

The formulated weighted Multi-Objective Function (MOF) combines both EVCCI and APLI and is given by

$$\text{MOF} = w_1 \cdot \text{EVCCI} + w_2 \cdot \text{APLI}, \tag{7}$$

where w_1 and w_2 are the weights assigned to EVCCI and APLI, respectively. Based on sensitivity analysis, their optimal values were determined to be 0.2 and 0.8.

B. System Constraints

1) Power Balance Constraints: To optimize the multi-objective function while ensuring real and reactive power balance, the following equations are applied:

$$P_{\text{grid}} + \sum_{n=1}^{N_{\text{dg}}} P_{\text{dg}} = \sum_{n=1}^{N_{\text{ul}}} P_d + \sum_{n=1}^{N_{\text{cs}}} P_{\text{cs}} + \sum_{n=1}^{N_{\text{BR}}} P_{\text{real}}, \tag{8}$$

$$Q_{\text{grid}} + \sum_{n=1}^{N_{\text{dg}}} Q_{\text{dg}} = \sum_{n=1}^{N_{\text{ul}}} Q_d + \sum_{n=1}^{N_{\text{cs}}} Q_{\text{cs}} + \sum_{n=1}^{N_{\text{BR}}} Q_{\text{reac}}, \tag{9}$$

where P_{grid} and Q_{grid} are the real and reactive power supplied by the grid; P_{dg} and Q_{dg} are the real and reactive power outputs of DG units; P_d and Q_d are the power demands at the u-node; P_{cs} and Q_{cs} are the real and reactive power demands of EVCS; and P_{real} and Q_{reac} are the active and reactive power losses in the m^{th} branch. The terms $N_{\text{dg}}, N_{\text{ul}}, N_{\text{cs}}$, and N_{BR} denote the number of DG units, load nodes, EVCS, and network branches, respectively. The forward/backward sweep algorithm [38] is used to solve these power flow equations efficiently in RDNs.

2) Voltage Constraints: To ensure power quality, the voltage at each node must remain within the permitted range:

$$0.95 \leq V_n \leq 1.05. \tag{10}$$

C. DG Constraints

The dispatchable real, reactive, and apparent power from DG units must lie within their operational limits, which are given by

$$P_{\text{dg}}^{\min} \leq P_{\text{dg},n} \leq P_{\text{dg}}^{\max}, \tag{11}$$

$$Q_{\text{dg}}^{\min} \leq Q_{\text{dg},n} \leq Q_{\text{dg}}^{\max}, \tag{12}$$

$$S_{\text{dg}}^{\min} \leq S_{\text{dg},n} \leq S_{\text{dg}}^{\max}, \tag{13}$$

where $P_{\text{dg}}^{\min}, Q_{\text{dg}}^{\min}, S_{\text{dg}}^{\min}$ are the minimum real, reactive, and apparent power limits, and $P_{\text{dg}}^{\max}, Q_{\text{dg}}^{\max}, S_{\text{dg}}^{\max}$ are their respective maximum values at bus n.

D. EVCS Constraints:

1) Charging Power Constraints: The power limits for standard and fast EV charging stations are constrained by

$$P_{\text{css}}^{\min} \leq P_{\text{css},k} \leq P_{\text{css}}^{\max}, \tag{14}$$

$$P_{\text{csf}}^{\min} \leq P_{\text{csf},k} \leq P_{\text{csf}}^{\max}, \tag{15}$$

where $P_{\text{css},k}$ and $P_{\text{csf},k}$ denote the real power ratings of SEVCS and FEVCS at bus k, respectively, and $P_{\text{css}}^{\min}, P_{\text{csf}}^{\min}$, $P_{\text{css}}^{\max}, P_{\text{csf}}^{\max}$ are their respective minimum and maximum ratings.

2) Charging Point (CP) Constraints: The number of fast and slow charging points must not exceed their maximum allowed values, as shown by

$$0 < F_{\text{cp}} \leq F_{\text{cp}}^{\max}, \tag{16}$$

$$0 < S_{\text{cp}} \leq S_{\text{cp}}^{\max}. \tag{17}$$

3) Charging Station (CS) Constraints: The number of fast and slow EVCS should also be within their respective limits:

$$0 < F_{\text{cs}} \leq F_{\text{cs}}^{\max}, \tag{18}$$

$$0 < S_{\text{cs}} \leq S_{\text{cs}}^{\max}. \tag{19}$$

4) EVCS Sizing Constraints: Finally, the total capacity of EVCS, denoted by TC_{cs}, is calculated using

$$TC_{\text{cs}} = N_{\text{cs}} \cdot C_{\text{cs}}, \tag{20}$$

where N_{cs} is the number of EVCS units and C_{cs} is the rated capacity of each EVCS.

III. Optimization Technique Adopted

The hybrid MWTLB-PSA is formed by the amalgamation of PSO and Weighted TLBO (WTLBO), and this technique is explained elaborately in this section. The main motive behind this hybridization is to ascertain a better search space and fast convergence. Also, it is identified that the minimal value of the objective function corresponding to the proposed technique is found to be less than that obtained when PSO and TLBO are applied separately.

A. Proposed Hybrid Technique

The proposed novel hybrid technique, including modifications, is explained in this section. PSO draws inspiration from environmental simulations, aiming to visually replicate the unpredictable movement patterns observed in bird flocks [21]. During each iteration, particle velocities adjust towards their 'pBest' and 'gBest' locations, with acceleration influenced by two distinct random numbers, and further velocity and position updates occur. Meanwhile, the WTLBO considers a portion of the learner's past value when calculating the new learner value, which is determined by a weight factor (w)[39]. Each learner receives support in various search abilities throughout the early phases of the local and global search using the WTLBO technique. The movement of the solutions is adjusted in later stages to reveal the underside of a comparatively tiny space where the overall predicted optimal solution is discovered.

B. Modification in the existing approach

In contrast to the original TLBO, the proposed WTLBO approach uses a weight factor (w) to determine the amount of the learner's previous value to be considered while computing the updated learner value. According to the algorithm, every person updates his/her location by the distance between the instructor in the teacher phase and the mean answer at least once or twice. Additionally, a student updates the location based on the distance from a randomly selected classmate. According to [23], a teacher can only raise pupils' grades by

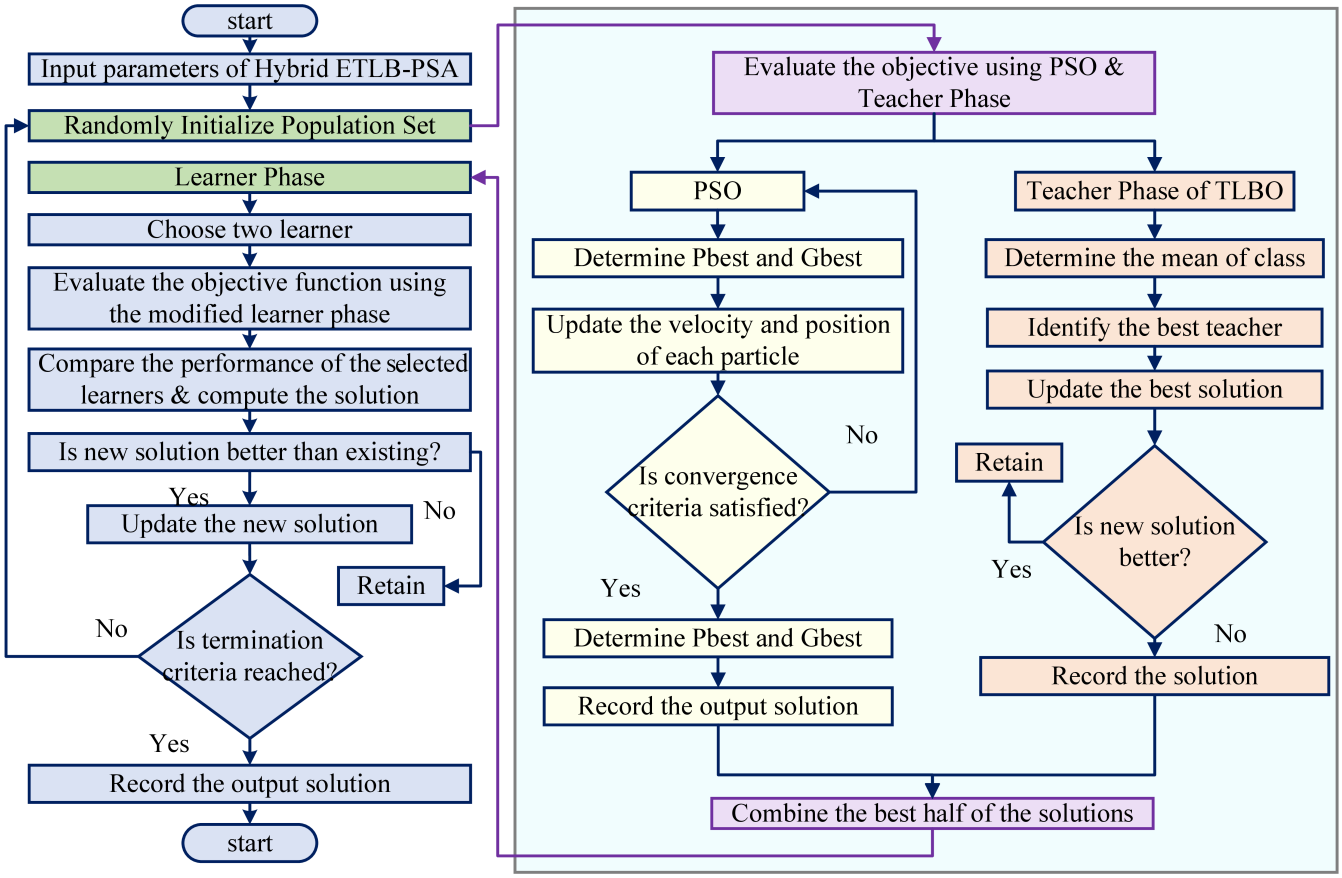

Fig. 3. Execution flow of the proposed Modified Weighted Teaching-Learning-Based Particle Swarm Algorithm (MWTLB-PSA).

calculating the class means. The distance between the teacher and the pupils is not considered during the teacher phase. In PSO, the gap between the person who is now the present best and the one who can assist the person raises their level of productivity. To increase the WTLBO algorithm's efficacy in learning, the PSO approach is used by WTLBO.

The updated learner position $X_{t,\text{new}}$ in the Modified Weighted Teaching-Learning Based PSO Algorithm is given by

$$X_{t,\text{new}} = w \cdot X_{t,\text{old}} + r_1 \cdot (X_{\text{teacher}} - T_f \cdot X_{\text{mean}}) + r_2 \cdot (X_{\text{teacher}} - X_{t,\text{old}}), \tag{21}$$

where $X_{t,\text{old}}$ is the current position of learner t, X_{teacher} is the best-performing solution (teacher), and X_{mean} is the average solution of the population. The variables r_1 and r_2 are random numbers uniformly distributed in the range $[0, 1]$, and T_f is the teaching factor.

The inertia weight w dynamically decreases over iterations and is computed as

$$w = \frac{\text{iter}_{\max} - \text{iter}}{\text{iter}_{\max}} \cdot (w_{\max} - w_{\min}) + w_{\min}, \tag{22}$$

where $w \in [0.8, 1.2]$, $\text{iter}_{\max}$ is the maximum number of iterations, and iter is the current iteration.

The teaching factor T_f, which controls the teaching effectiveness in a given iteration, is defined by

$$T_f = \text{round}(1 + \text{rand}(0, 1)). \tag{23}$$

The learner phase of the proposed Modified Weighted TLBO algorithm is detailed in the following pseudocode.

Algorithm 1 Learner Phase of MWTLB-PSA

```
for i = 1 to pop do
    Randomly select two learners X_t and X_j
    if f(t) < f(j) then
        X_{i,new} = w · X_{i,old} + r_3 · (X_t − X_j)
    else
        X_{i,new} = w · X_{i,old} + r_4 · (X_j − X_t)
    end if
end for
```

Here, r_3 and r_4 are random numbers uniformly distributed in the interval $[0, 1]$; X_t and X_j are positions of two randomly selected learners; and $f(t)$, $f(j)$ are their respective fitness values. The updated position $X_{i,\text{new}}$ is derived by moving toward the better-performing peer.

C. Proposed Hybrid Modified Weighted Teaching Learning Based Particle Swarm Algorithm (MWTLB-PSA)

The method initializes the population at random in the beginning. The PSO algorithm also initializes a random set of populations at the initial stage. These are the initial sets of individuals that serve as an initial population for the WTLBO algorithm's teacher phases and PSO, respectively. Half of the

most outstanding population acquired during the teacher phase is fed into the learner phase of WTLBO, together with the finest half collected during the PSO. At last, the entire population matches the basic population, bringing the first cycle to an end. Convergence is tested at the upgraded population of the learner phase. The convergence criterion is fixed as follows: The difference between the objective function value of any two consecutive iterations is checked for being less than a tolerance value of 1×10^{-6}. If so, then the convergence is considered to be satisfied, and the loop is exited. The flowchart explaining the entire flow of the proposed method is displayed in Fig. 3. The findings show that, in comparison to [14] and [21], the suggested approach finds the objective function with greater performance and lesser computing time, evident from section IV.

D. Uniqueness of hybrid MWTLB-PSA

The computing expense of initializing hybrid MWTLB-PSA for an optimization problem with m choice variables is $O(N_m)$, where N is the number of population members. Every iteration updates the positions in the search area in two stages. Consequently, the objective function for each individual in the population is calculated twice during every iteration. As a result, the population update procedure has a computational complexity of $O(2N_m t)$, where t is the total number of iterations. Based on this, the suggested strategy has a total computing burden of $O(N_m(2t+1))$, while that of PSO is $O(N_m(t+1))$. As a result, the suggested technique has double the computational burden of PSO but identical circumstances to WTLBO in terms of computational complexity. However, in hybrid MWTLB-PSA & WTLBO, the number of function evaluations in each iteration is equal to $2N$, but in PSO, it is equal to N. This makes the proposed algorithm unique in its feature of fast computing time with better search techniques. This has also been found to minimize the chances of local solutions.

IV. Results and Discussions

A 25-node RN is superimposed onto the IEEE 33-bus RDN to design an efficient layout for the charging station. The superimposed test system is illustrated in Fig. 4, which shows the geographical overlay of a 25-node urban RN (bottom, colored in blue) and a 33-bus RDN (top, shaded in pink). Starting with bus 1, the RDN is organized like a tree, with branching routes connecting to other buses like 19–22, 23–25, and 26–33. The RN, on the other hand, simulates actual vehicle routing and movement patterns by forming a connected structure with many route alternatives connecting the nodes. To support holistic planning of EVCS and DGs, nodes 2–18, 19–22, 23–25, and 26 in the RDN are highlighted using the same color scheme as nodes 1–17, 18–21, 22–24, and 25 in the RN which represent the superimposed nodes as listed in table II. The source of RDN data is [14]. The weights and distance data for RN are taken from [40].

The projected EV population at the RN nodes, obtained from [32], is estimated at 238 vehicles, and all 25 nodes are treated as demand points in this study. The proposed method is

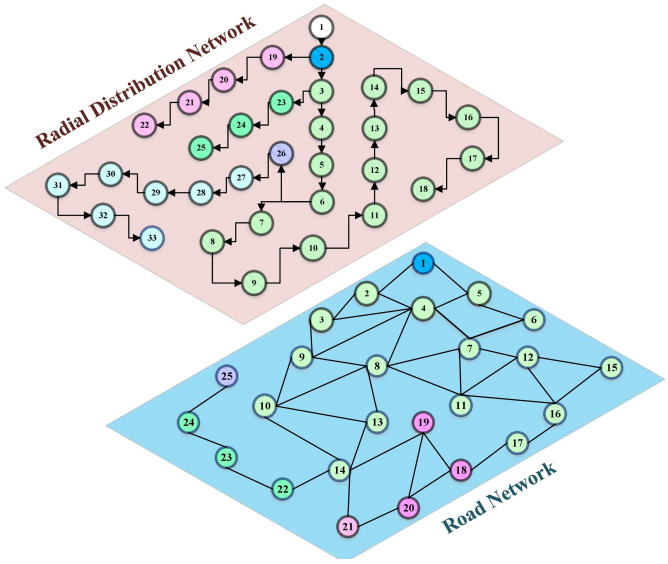

Fig. 4. Superimposed layout of the IEEE 33-bus RDN and 25-node RN used for EVCS and DG planning.

evaluated using a population size of 100, with the parameters $C_1 = C_2 = 2$, $w_{\min} = 0.4$, $w_{\max} = 0.9$ [41]. The algorithm iterates until the convergence criterion is met, maintaining a precision tolerance of 1×10^{-6}. Computations are performed using MATLAB 2022b on a Windows 10 system with 4GB RAM. As per the categorization in [14], the 32 buses (except the slack bus) of the RDN are divided into constant power, residential, industrial, and commercial load types. Since RN nodes 1–25 overlap with RDN nodes 2–26, the analysis exclusively considers buses 2–26 for the placement problem.

TABLE II
Superimposed Nodes of RDN and RN

RDN	2	3	4	5	6	7	8
RN	1	2	3	4	5	6	7
RDN	9	10	11	12	13	14	15
RN	8	9	10	11	12	13	14
RDN	16	17	18	19	20	21	22
RN	15	16	17	18	19	20	21
RDN	23	24	25	26	-	-	-
RN	22	23	24	25	-	-	-

To enhance customer experience and optimize utilization, this strategy integrates both SEVCS and FEVCS. By analyzing, the plan determines the ideal placement and sizing tailored to regional demands. SEVCS are allocated to support buses in the constant residential zone (Z1), and FEVCS is planned to integrate into commercial and industrial zones (Z2 and Z3). The zonal separation of the buses is provided in Table III. This work considers a base case along with three additional scenarios to evaluate the performance. To assess the effectiveness of the proposed algorithm, the outcomes from all three cases are systematically compared against those obtained using the existing algorithm.

- **Base case:** The base scenario involves determining APL by performing a load flow on the RDN without integrating EVCS and DG.

TABLE III
PARTITION OF REGIONS BASED ON THE LOAD TYPE

Zones	Load type	Buses covered
Z1	Residential zone	2, 3, 4, 5, 19, 20, 21, 22, 23, 24, 25
Z2	Industrial load	6, 7, 8, 9, 10, 11, 12, 13, 14, 15, 16, 17, 18
Z3	Commercial load	26, 27, 28, 29, 30, 31, 32, 33

- **Case 1:** In this scenario, the highest possible APL variation and EV consumer cost are reduced by strategically placing and scaling EVCS on the overlaid network.
- **Case 2:** In this scenario, the DGs are sized and positioned optimally in this system integrated with EVCS to reduce APL and the cost to the EV customer.
- **Case 3:** In order to reduce APL and EV consumer costs, EVCS and DGs are placed and sized concurrently.

A. Base Case

The forward and backward sweep method is used for load flow analysis since the test system is radial and has a large R/X ratio. The base values are recorded as APL of 202.7 kW, RPL of 135.51kvar, and minimum bus voltage of 0.9131 p.u.

B. Case1: Integration of EVCS

Case 1 focuses on the optimal placement and sizing of EVCS. The placement of EVCS is determined by considering superimposed nodes, with the nearest EVCS to the demand point selected to minimize EV consumer costs. Following the placement, the test system's losses and voltage levels are calculated using the distribution load flow algorithm. The optimization process employs the MWTLB-PSA technique to address the multi-objective function effectively. The results are compared with the existing HTLBO-PSO and PSO techniques, as detailed in [14] and [21].

Table IV outlines the input parameters for EVCS placement using both approaches, including data on obtained S_{cp}^{max}, F_{cp}^{max}, S_{cs}^{max}, and F_{cs}^{max} from [9]. Table V presents the locations, ratings, and their impact on the RDN using both algorithms. The results indicate that the MWTLB-PSA technique identifies EVCS locations at nodes 4, 8, 20, and 23 with ratings of 230.4 kW, 600 kW, 76.8 kW, and 153.6 kW, respectively. Similarly, the EVCS locations and ratings derived from the HTLBO-PSO and PSO techniques are also listed in Tables IV and V. The findings highlight the significant influence of EVCS placement and sizing on the performance of the RDN.

When EVCSs are integrated into the RDN, APL is observed to be 252.71 kW with the MWTLB-PSA technique, compared to 271.01 kW and 304.71 kW using the HTLBO-PSO and PSO approach, respectively. This represents an increase in APL by 19.79% %, 25.2%, and 33.47% from the base case for MWTLB-PSA, HTLBO-PSO, and PSO, respectively, as shown in Fig. 5(a) and Table IV. Similarly, RPL increased by 18.3% (from 135.51 kvar to 165.88 kvar) with MWTLB-PSA, 24.44% (from 135.51 kvar to 179.34 kvar) with HTLBO-PSO, and 34.76% (from 135.51 kvar to 207.73 kvar) by PSO as depicted in Fig. 5(b) and Table IV. These results demonstrate that the MWTLB-PSA technique results in significantly lower losses compared to the HTLBO-PSO and PSO techniques, emphasizing its superior efficiency in optimizing EVCS placement and sizing

The deployment of EVCS results in a system minimum voltage drop of 0.9131 p.u. (base case) to 0.9048 p.u. using MWTLB-PSA, 0.8964 p.u. with HTLBO-PSO, and 0.8764 p.u. using PSO. Figures 6 (a), 6(b), and 6(c) illustrate the voltage variation for various algorithms. Additionally, Fig. 7(a) highlights that the EVCCI is 0.5425 for MWTLB-PSA, 0.7714 for HTLBO-PSO, and 0.8739 for PSO, indicating that MWTLB-PSA demonstrates faster evolution compared to HTLBO-PSO and PSO. DG units are strategically deployed to counteract the impacts of EVCS integration on the RDN.

C. Case2: Integration of DG units

In this scenario, DG units are integrated into a system already equipped with EVCS (as analyzed in Case 1). Adding DG units significantly reduces losses and enhances the voltage profile within the RDN. The analysis reveals that incorporating four DG units yields better results than deploying one, two, or three units, with negligible improvements observed beyond four DGs [14]. Hence, this study considers integrating four DG units, adhering to the network's overall kVA capacity limits to define the minimum and maximum ratings for each unit.

Table V presents the optimal results for the DG placement and various technical observations for both algorithms. The proposed technique has identified buses 3, 9, 21, and 25 as optimal locations for DG integration, with corresponding ratings of 2371.2 kVA, 1968.36 kVA, 819.7 kVA, and 161.23 kVA, respectively. With the introduction of DG units, the APL reduced by 71.89% (from 252.71 kW to 71.01 kW) using MWTLB-PSA, compared to a 48.52% reduction achieved with HTLBO-PSO and 40% reduction achieved with PSO, as depicted in Fig. 5(a). Similarly, Fig. 5(b) shows a reduction in RPL of 68.15% (from 165.88 kvar to 52.90 kvar) with MWTLB-PSA, 42.11% (from 179.34 kvar to 103.82 kvar) with HTLBO-PSO, and 35.61% (from 207.73 kvar to 133.75 kvar) with PSO. These findings confirm that the MWTLB-PSA technique outperforms HTLBO-PSO and PSO by achieving greater reductions in both APL and RPL, demonstrating its superior effectiveness in optimizing DG placement and sizing.

Furthermore, the minimum bus voltage is improved to 0.9825 p.u. from 0.9048 p.u. at bus no. 18 using MWTLB-PSA. The variation shown in Fig. 6(a), 6(b), and 6(c) displays the improvement of voltage in the 18th bus to 0.9500 p.u. from 0.8964 p.u. using HTLBO-PSO and from 0.8764 p.u. to 0.9500 p.u. using PSO, respectively. This progress can be attributed to the correct positioning of the DGs. MWTLB-PSA generated effective results faster than HTLBO-PSO and PSO.

D. Case 3: Simultaneous Placement of DG and EVCS

Simultaneous EVCSs and DGs planning are carried out using both the MWTLB-PSA and HTLBO-PSO methods. The design of EVCS is summarized in Table VII. Initially, the locations and sizes of both EVCS and DG units are

TABLE IV
EVCS INPUT DATA FOR CASE 1

Parameters	MWTLB-PSA				HTLBO-PSO				PSO			
EVCS location	4	8	20	23	5	15	20	23	2	8	21	26
Rating of charging points (kW)	19.2	50	19.2	19.2	19.2	50	19.2	19.2	19.2	50	19.2	19.2
No of charging points per EVCS	6	4	4	4	5	5	4	5	6	4	2	3
Rating of EVCS (kW)	115.2	200	76.8	76.8	96	250	76.8	96	115.2	200	34.8	57.6
No of EVCS	2	2	1	2	2	2	2	2	3	2	3	4
Total rating (kW)	230.4	400	76.8	153.6	192	500	153.6	192	345.6	400	115.2	230.4
Multi-Objective Function	0.7373				0.8010				0.8475			
Run Time (sec)	9.461				16.049				17.367			

TABLE V
OPTIMAL LOCATION AND SIZING OF EVCSS WITHOUT DGS IN RADIAL DISTRIBUTION SYSTEM

Parameters	MWTLB-PSA				HTLBO-PSO				PSO			
EVCS location	4	8	20	23	5	15	20	23	2	8	21	26
EVCS rating (kW)	230.4	600	76.8	153.6	192	500	153.6	192	345.6	400	115.2	230.4
APL (kW) (%Reduction)	252.71 (24.67%)				271.01(33.7%)				304.71 (50.32%)			
RPL (kvar)(%Reduction)	165.88 (22.41%)				179.34 (32.34%)				207.73(53.29%)			
Minimum voltage (p.u.)	0.9048 at bus no 18				0.8964 at bus no 18				0.8764 at bus no 18			
EV Consumer Cost Index	0.5425				0.7714				0.8739			

TABLE VI
OPTIMAL LOCATION AND SIZING OF EVCSS WITH INTEGRATION OF DGS IN RADIAL DISTRIBUTION SYSTEM

Parameters	MWTLB-PSA				HTLBO-PSO				PSO			
EVCS location	4	8	20	23	5	15	20	23	2	18	21	26
EVCS rating (kW)	230.4	600	76.8	153.6	192	500	153.6	500	345.6	400	115.2	230.4
DG location	3	9	21	25	3	14	19	24	3	10	24	29
DG rating (kVA)	2371.2	1958.36	819.7	161.23	991.53	470.12	24.79	3008.72	1702.9	51.63	591.9	283.34
APL (kW) (% Reduction)	71.01 (71.89%)				139.50 (48.52%)				182.82 (40%			
RPL (kvar)(% Reduction)	52.90(68.15%)				103.82 (42.11%)				133.75 (35.61%)			
Minimum voltage (p.u.)	0.9825 at bus no 18				0.9500 at bus no 18				0.9500 at bus no 18			
EV Consumer Cost Index	0.5425				0.7714				0.8739			
Multi Objective Function	0.5711				0.6696				0.9775			
Run Time (sec)	7.072				10.995				16.181			

incorporated. Once these are added, the system is evaluated to determine the improvement in the overall objective function, and the results are displayed in Table VIII.

The APL for the network is found to be 57.75 kW using the MWTLB-PSA method, 99.08 kW using HTLBO-PSO, and 132.71 kW using PSO, as shown in Fig. 5(a). The concurrent placement of EVCS and DG units results in a reduced RPL. As shown in Fig.5(b), MWTLB-PSA yields a total RPL of 44.42 kvar, while HTLBO-PSO and PSO result in 72.99 kvar and 94.31 kvar, respectively. These results indicate that MWTLB-PSA outperforms HTLBO-PSO and PSO in reducing power losses. Fig. 6 (a), 6(b), and 6(c) reveal improvements in the voltage profile of the RDN with simultaneous allocation of EVCS and DG units. MWTLB-PSA improves the voltage profile to 0.9887 p.u., while HTLBO-PSO and PSO achieve 0.9807 p.u. and 0.9585 p.u. Respectively. Furthermore, the EVCCI is reduced to 0.3958 using MWTLB-PSA, compared to 0.4423 using HTLBO-PSO and 0.7300 using PSO, as seen in Fig. 7(a). The schematic representation of the optimal placement of EVCS and DG units in each zone of the IEEE 33 bus RDN is displayed in Fig. (b). Thus, it is concluded that MWTLB-PSA not only simulates faster but also yields superior results with fewer iterations, making it a more efficient method for simultaneous EVCS and DG planning.

TABLE VII
EVCS INPUT DATA FOR CASE 3

Parameters	MWTLB-PSA				HTLBO-PSO				PSO			
EVCS location	5	8	20	23	3	15	20	23	5	9	21	26
Rating of charging points (kW)	19.2	50	19.2	19.2	19.2	50	19.2	19.2	19.2	500	19.2	19.2
No of charging points per EVCS	4	6	4	4	7	6	9	5	7	6	3	5
Rating of EVCS (kW)	76.8	300	76.8	76.8	134.4	300	172.8	96	134.4	300	57.6	96
No of EVCS	2	2	2	2	2	2	1	1	2	2	3	2
Total rating (kW)	153.6	600	153.6	153.6	268.8	600	172.8	96	268.8	600	172.8	192
Multi-Objective Function	0.477				0.7202				0.7821			
Run Time (sec)	5.914				8.787				8.90			

TABLE VIII
OPTIMAL LOCATION AND SIZING OF EVCSS, SIMULTANEOUS PLANNING OF EVCS AND DG UNITS

Parameters	MWTLB-PSA	HTLBO-PSO	PSO
EVCS location	5, 8, 20, 23	3, 15, 20, 23	5, 9, 21, 26
EVCS rating (kW)	153.6, 600, 153.6, 153.6	268.8, 600, 172.8, 96	268.8, 600, 172.8, 192
DG location	4, 9, 19, 24	2, 9, 21, 24	2, 14, 20, 23
DG rating (kVA)	2878.92, 809.12, 511.38, 1457.67	1900.6, 263.3, 973.8, 1394.9	254.6, 853.6, 739.6, 2335.2
APL (kW) (% Reduction)	57.75 (77.14%)	96.86 (64..25%)	132.71 (56.44%)
RPL (kvar) (% Reduction)	44.82 (72.89%)	71.69 (60.02%)	94.31 (54.59%)
Minimum voltage (p.u.)	0.9887 at bus no 18	0.9620 at bus no 18	0.9585 at bus no 18
EVCCI	0.3958	0.4423	0.7300

E. Economic Analysis

The planning problem is further subjected to the economic analysis [9], which involves the installation cost of EVCS as expressed in the given equation.

$$C_{\text{installation}} = \left(\sum_{i=1}^{N} (F_{cp} \times F_{cs}) \times c_f\right) + \left(\sum_{i=1}^{N} (S_{cp} \times S_{cs}) \times c_s\right) \tag{24}$$

It is inferred that the installation cost ($C_{\text{installation}}$) depends on the cost of installing fast (c_f) and slow (c_s) chargers, including the number of fast chargers F_{cs} and slow chargers S_{cs}, as well as the number of fast and slow charging points F_{cp} and S_{cp} [9]. The outcome is depicted in Fig. 8. It is observed that the installation cost of EVCS using the proposed method accounts for \$2.95 million, which is considered to be economical compared to \$3.14 million and \$3.38 million obtained using HTLBO-PSO and PSO, respectively.

F. Sensitivity Analysis of the Proposed Method

The sensitivity of the proposed algorithm due to parameter variation is presented in Fig. 9. The weights (w_1) correspond to the weightage given to the consumer cost index (EVCCI), and (w_2) corresponds to the weightage given to the active power loss index (APLI). The objective function formulated is evaluated using MWTLB-PSA for different ranges of weights (w_1, w_2) such that $\sum_{i=1}^{n} w_i = 1$. For every combination of the weights, the objective function is computed in every iteration, and the solution corresponding to the minimal value is considered the best solution. This is repeated as an outer loop for every iteration, and the sensitivity is analyzed. It is observed that the minimum objective value is subject to change depending on the weights for every iteration, and the values are plotted in Fig.9. The minimum objective function value is obtained when $w_1 = 0.2$ and $w_2 = 0.8$.

G. Highlights of the Proposed Methodology

A detailed comparison of the performance of the proposed methodology against various methods used in references is depicted in Table IX, which illustrates the remarkable efficiency of the proposed MWTLB-PSA method in arriving at the optimal location and sizing of the EVCSs and DGs at the 33-bus RDN, outperforming several state-of-the-art algorithms, including hybrid TLBO-PSO, EHO, PSO, HHO, TLBO, and index-based methods. The MWTLB-PSA achieves the lowest APL of 57.75 kW and ensures a minimum voltage of 0.9887 p.u., reflecting its superior capability in enhancing voltage stability and minimizing power losses. Furthermore, the method demonstrates its robustness in minimizing the EVCCI, achieving an impressive value of 0.3958, along with the installation cost of \$2.95 million as shown in Fig. 8, which is significantly better than other algorithms such as PSO and CSO-TLBO, respectively. These results underscore the effectiveness of MWTLB-PSA in addressing the challenges of distribution system optimization. Moreover, the sensitivity

TABLE IX
COMPARISON OF VARIOUS TECHNIQUES FOR APL, MINIMUM VOLTAGE, EVCCI, AND INSTALLATION COST

Ref. No	Year	Technique	APL (kW)	Minimum voltage (p.u.)	EVCCI	Installation cost (millions of $)
[15]	2023	HTLBO-PSO	72.56	0.9527	-	-
[16]	2020	HHO, TLBO	67.56	0.9586	-	-
[18]	2019	EHO	78.4	0.9386	-	-
[19]	2020	Index Based	67.4	0.9535	-	-
[21]	2021	PSO	64.91	0.9611	-	-
[27]	2020	HHO, TLBO	68.07	0.9685	-	-
[32]	2023	PSO	-	-	0.4525	-
[9]	2019	CSO-TLBO	-	-	-	3.026-3.607
Proposed MWTLB-PSA			57.75	0.9887	0.3958	2.95

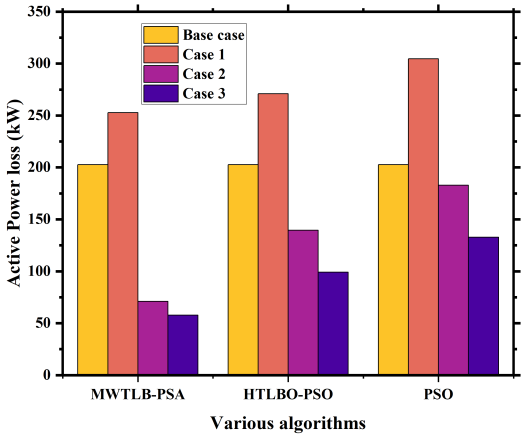

(a)

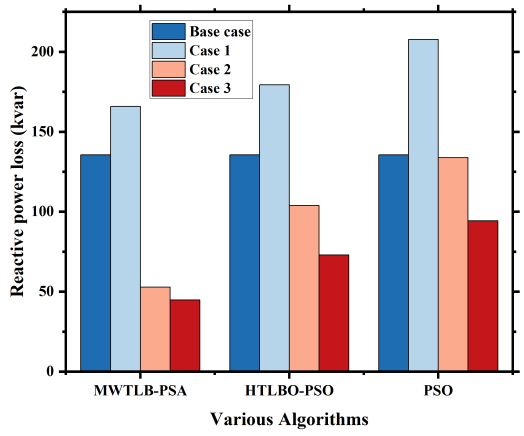

(b)

Fig. 5. Power Loss Variations for Different Cases: (a) Active Power Loss and (b) Reactive Power Loss.

analysis is also performed to record the sensitivity of the objective function with respect to weights, as depicted in Fig.9.

The authors further emphasize the exceptional performance of the proposed MWTLB-PSA method through detailed comparisons with hybrid algorithms in Tables I to VIII, which showcase the best solutions achieved by existing approaches. Notably, Scenario 3 achieves outstanding results using MWTLB-PSA, surpassing the HTLBO-PSO and PSO methods. This is further visualized in Fig. 6(b), which depicts the optimal placement of EVCS and DG achieved by the proposed approach. The consistent success of MWTLB-PSA across various scenarios highlights its robustness, adaptability, and strong potential for effectively optimizing large-scale RDN. The suggested approach is intended to be adaptable and scalable, even though it has been evaluated on common test systems such as the IEEE 33-bus RDN overlaid with a 25-node RN. Due to its design, the algorithm can manage increasingly complex and large electrical and transportation networks without sacrificing efficiency. As the system size increases, the hybrid optimization framework continues to exhibit significant convergence properties. As a result, the technique is appropriate for real-world applications and can be successfully implemented in both small and large networks.

V. CONCLUSION

This paper has proposed an innovative planning strategy that integrates DG and EVCS to mitigate voltage variations, reduce power losses, and lower costs for EV users within a connected network. Three distinct scenarios are analyzed for optimal EVCS planning: i) EVCS alone, ii) optimal DG unit placement based on prior EVCS configurations, and iii) a combined approach for simultaneous planning of both EVCS and DG units. The proposed planning framework incorporates an overlaid road and distribution network, reflecting real-world conditions for practical implementation. To improve the planning process, an enhanced MWTLB-PSA is introduced, which addresses the discrepancy between the best individual solutions and the refinement process. This enhancement allows the algorithm to converge more quickly and perform more effectively. The proposed algorithm achieves an APL of 57.75 kW (77.14% reduction) and an improved EVCCI of 0.3958 compared to existing techniques. Furthermore, it consistently yields the best solution in terms of voltage profile improvement compared to other state-of-the-art optimization algorithms. With MWTLB-PSA, the simultaneous planning of the EVCS and DG units achieves faster convergence and superior performance. Future studies could examine the stochastic character of both EVCS and DG, assessing the influence on the simultaneous planning of both EVCS and DG under unpredictable generation patterns.

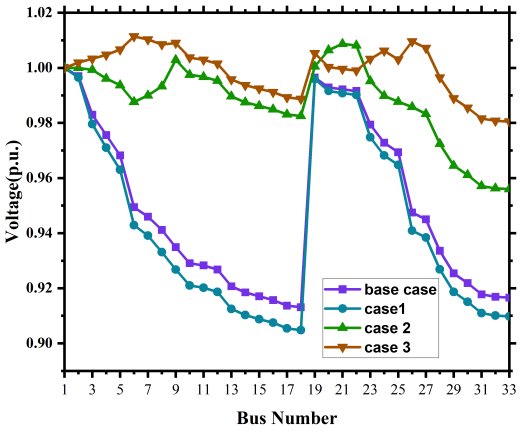

(a)

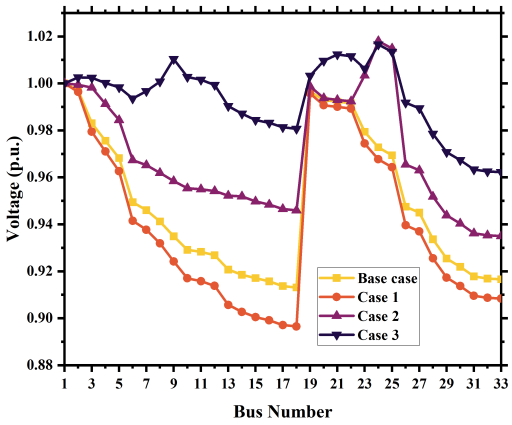

(b)

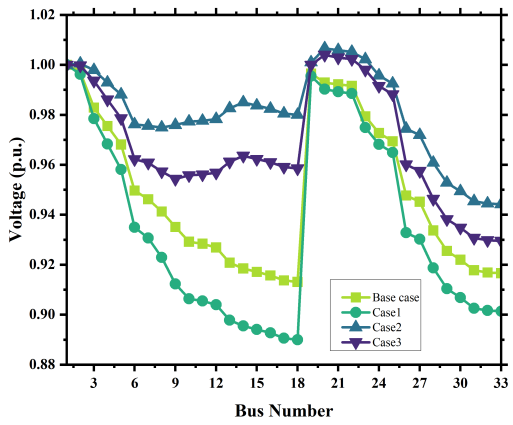

(c)

Fig. 6. Voltage Magnitude Variations for Different Cases: (a) Using MWTLB-PSA (b) Using HTLBO-PSO and (c) Using PSO.

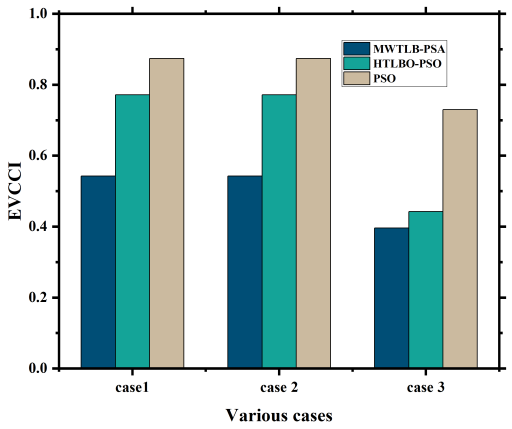

(a)

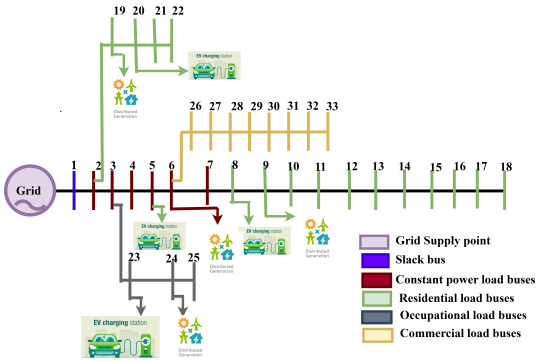

(b)

Fig. 7. EVCS and DG Analysis for 33 RDN: (a) Variation of EVCCI and (b) Schematic Representation of Optimal Placement.

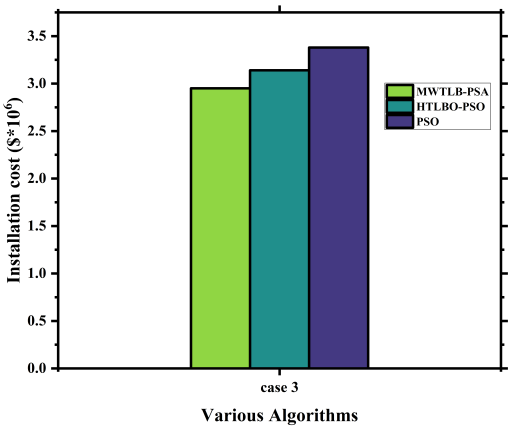

Fig. 8. Economic analysis of EVCS installation costs using different optimization algorithms.

REFERENCES

[1] F. Knobloch, S. Hanssen, A. Lam, et al., "Net emission reductions from electric cars and heat pumps in 59 world regions over time," Nature Sustainability, vol. 3, no. 6, pp. 437–447, 2020, doi: 10.1038/s41893-020-0488-7.

[2] R. Zhang and S. Fujimori, "The role of transport electrification in global climate change mitigation scenarios," Environmental Research Letters, vol. 15, no. 3, p. 034019, 2020, doi: 10.1088/1748-9326/ab6658.

[3] International Energy Agency (IEA), "Global EV Outlook 2018," IEA, Paris, 2018. [Online]. Available: https://www.iea.org/reports/global-ev-outlook-2018

[4] G. Saldaña, J. I. San Martin, I. Zamora, F. J. Asensio, and O. Oñederra, "Electric vehicle into the grid: Charging methodologies aimed at providing ancillary services considering battery degradation," Energies, vol. 12, no. 12, p. 2443, 2019, doi: 10.3390/en12122443.

[5] T. U. Solanke, V. K. Ramachandaramurthy, J. Y. Yong, J. Pasupuleti, P. Kasinathan, and A. Rajagopalan, "A review of strategic charging–discharging control of grid-connected electric vehicles," Journal of Energy Storage, vol. 28, p. 101193, 2020, doi:

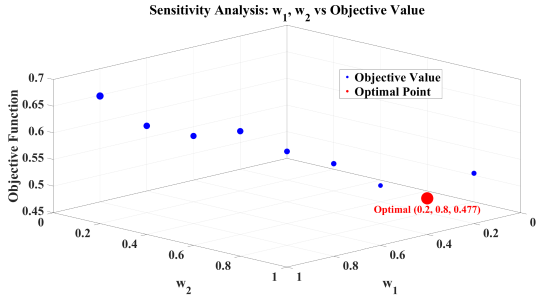

Fig. 9. Sensitivity analysis of the objective function with various weights.

10.1016/j.est.2020.101193.

[6] R. S. Gupta, A. Tyagi, and S. Anand, "Optimal allocation of electric vehicles charging infrastructure, policies and future trends," Journal of Energy Storage, vol. 43, p. 103291, 2021, doi: 10.1016/j.est.2021.103291.

[7] M. H. Ghodusinejad, Y. Noorollahi, and R. Zahedi, "Optimal site selection and sizing of solar EV charge stations," Journal of Energy Storage, vol. 56, p. 105904, 2022, doi: 10.1016/j.est.2022.105904.

[8] X. Guo, Z. Bao, H. Lai, and W. Yan, "Model predictive control considering scenario optimisation for microgrid dispatching with wind power and electric vehicle," The Journal of Engineering, vol. 2017, no. 13, pp. 2539–2543, 2017, doi: 10.1049/joe.2017.0785.

[9] S. Deb, K. Tammi, K. Kalita, and P. Mahanta, "Charging Station Placement for Electric Vehicles: A Case Study of Guwahati City, India," IEEE Access, vol. 7, pp. 100270–100282, 2019, doi: 10.1109/ACCESS.2019.2931055.

[10] Z. H. Zhu, Z. Y. Gao, J. F. Zheng, and H. M. Du, "Charging station location problem of plug-in electric vehicles," Journal of Transport Geography, vol. 52, pp. 11–22, 2016, doi: 10.1016/j.jtrangeo.2016.02.002.

[11] W. Yao et al., "A Multi-Objective Collaborative Planning Strategy for Integrated Power Distribution and Electric Vehicle Charging Systems," in IEEE Transactions on Power Systems, vol. 29, no. 4, pp. 1811-1821, July 2014, doi: 10.1109/TPWRS.2013.2296615.

[12] Rawa, Muhyaddin, et al. "Economical-technical-environmental operation of power networks with wind-solar-hydropower generation using analytic hierarchy process and improved grey wolf algorithm," Ain Shams Engineering Journal, vol. 12, no. 3, pp. 2717–2734, 2021, doi: 10.1016/j.asej.2021.02.004.

[13] Clairand, Jean-Michel, et al. "Optimal siting and sizing of electric taxi charging stations considering transportation and power system requirements," *Energy*, vol. 256, p. 124572, 2022, doi: 10.1016/j.energy.2022.124572.

[14] D. B. R and V. M, "Allocation of EV Charging Stations in a Microgrid," 2023 IEEE International Conference on Energy Technologies for Future Grids (ETFG), Wollongong, Australia, 2023, pp. 1-6, doi: 10.1109/ETFG55873.2023.10408134.

[15] A. Pal, A. Bhattacharya and A. K. Chakraborty, "Allocation of EV Fast Charging Station with V2G Facility in Distribution Network," 2019 8th International Conference on Power Systems (ICPS), Jaipur, India, 2019,pp. 1-6, doi: 10.1109/ICPS48983.2019.9067574.

[16] P. V. K. Babu and K. Swarnasri, "Optimal integration of different types of DGs in radial distribution system by using Harris hawk optimization algorithm," Cogent Engineering, vol. 7, no. 1, p. 1823156, 2020, doi: 10.1080/23311916.2020.1823156.

[17] G. V. N. Lakshmi, A. Jayalaxmi, and V. Veeramsetty, "Optimal placement of distribution generation in radial distribution system using hybrid genetic dragonfly algorithm," Technology and Economics of Smart Grids and Sustainable Energy, vol. 6, pp. 1–13, 2021, doi: 10.1007/s40866-021-00107-w.

[18] C. H. Prasad, K. Subbaramaiah, and P. Sujatha, "Cost–benefit analysis for optimal DG placement in distribution systems by using elephant herding optimization algorithm," Renewables: Wind, Water, and Solar, vol. 6, no. 1, p. 2, 2019, doi: 10.1186/s40807-019-0056-9.

[19] G. Memarzadeh and F. Keynia, "A new index-based method for optimal DG placement in distribution networks," Engineering Reports, vol. 2, no. 10, p. e12243, 2020, doi: 10.1002/eng2.12243.

[20] A. Kumar, R. Verma, N. K. Choudhary, and N. Singh, "Optimal placement and sizing of distributed generation in power distribution system: A comprehensive review," Energy Sources, Part A: Recovery, Utilization, and Environmental Effects, vol. 45, no. 3, pp. 7160–7185, 2023, doi: 10.1080/15567036.2023.2216167.

[21] Haider, Waseem, et al."Voltage profile enhancement and loss minimization using optimal placement and sizing of distributed generation in reconfigured network," Machines, vol. 9, no. 1, p. 20, 2021, doi: 10.3390/machines9010020.

[22] Selim, Ali, et al. "Optimal allocation of multiple types of distributed generations in radial distribution systems using a hybrid technique," Sustainability, vol. 13, no. 12, p. 6644, 2021, doi: 10.3390/su13126644.

[23] A. Zabihia and M. Parhamfarb, "Empowering the grid: Toward the integration of electric vehicles and renewable energy in power systems," International Journal of Energy Security and Sustainable Energy, vol. 2, no. 1, pp. 1–14, 2024, doi: 10.5281/zenodo.12751722.

[24] M. Parhamfar and A. Zabihi, "Decentralized energy solutions: The impact of smart grid-enabled EV charging stations," SSRN, 2024, doi: 10.2139/ssrn.4961812. [Online].

[25] A. Zabihi and M. Parhamfar, "Decentralized energy solutions: The impact of smart grid-enabled EV charging stations," Heliyon, 2025, doi: 10.1016/j.heliyon.2025.e41815.

[26] B. V. Kumar and A. F. M A, "Optimal Integration of EV Charging Stations and Capacitors for Net Present Value Maximization in Distribution Network," in IEEE Latin America Transactions, vol. 23, no. 3, pp. 239-250, March 2025, doi: 10.1109/TLA.2025.10879176

[27] V. K. B. Ponnam and K. Swarnasri, "Multi-objective optimal allocation of electric vehicle charging stations and distributed generators in radial distribution systems using metaheuristic optimization algorithms," Engineering, Technology & Applied Science Research, vol. 10, no. 3, pp. 5837–5844, 2020, doi: 10.48084/etasr.3517.

[28] Ahmad, Fareed, et al. "Placement of electric vehicle fast charging stations in distribution network considering power loss, land cost, and electric vehicle population," Energy Sources, Part A: Recovery, Utilization, and Environmental Effects, vol. 44, no. 1, pp. 1693–1709, 2022, doi: 10.1080/15567036.2022.2055233.

[29] M. Bilal, F. Ahmad, and M. Rizwan, "Techno-economic assessment of grid and renewable powered electric vehicle charging stations in India using a modified metaheuristic technique," Energy Conversion and Management, vol. 284, p. 116995, 2023, doi: 10.1016/j.enconman.2023.116995.

[30] R. Chakraborty, D. Das and P. Das, "Optimal Placement of Electric Vehicle Charging Station with V2G Provision using Symbiotic Organisms Search Algorithm," 2022 IEEE International Students' Conference on Electrical, Electronics and Computer Science (SCEECS), BHOPAL, India, 2022, pp. 1-6, doi: 10.1109/SCEECS54111.2022.9740988.

[31] A.-M. Hariri, M. A. Hejazi, and H. Hashemi-Dezaki, "Reliability optimization of smart grid based on optimal allocation of protective devices, distributed energy resources, and electric vehicle/plug-in hybrid electric vehicle charging stations," Journal of Power Sources, vol. 436, p. 226824, 2019, doi: 10.1016/j.jpowsour.2019.226824.

[32] V. Vutla, V. Chintham, and V. K. D. Mallesham, "Meta heuristic algorithm based multi-objective optimal planning of rapid charging stations and distribution generators in a distribution system coupled with transportation network," Advances in Electrical & Electronic Engineering, vol. 20, no. 4, 2022, doi:10.15598/aeee.v20i4.4594.

[33] H. A. Rad, M. Jafari-Nokandi, and S. M. Hosseini, "Optimal allocation of plug-in electric vehicle parking lots for maximum serviceability and profit in the coupled distribution and transportation networks," Scientia Iranica. Transaction D, Computer Science & Engineering, Electrical, vol. 31, no. 14, pp. 1178–1196, 2024, doi: 10.24200/sci.2022.58500.5768.

[34] A. Shukla, K. Verma, and R. Kumar, "Multi-objective synergistic planning of EV fast-charging stations in the distribution system coupled with the transportation network," IET Generation, Transmission & Distribution, vol. 13, no. 15, pp. 3421–3432, 2019, doi: 10.1049/iet-gtd.2019.0486.

[35] P. Skaloumpakas, E. Spiliotis, E. Sarmas, A. Lekidis, G. Stravodimos, D. Sarigiannis, I. Makarouni, V. Marinakis, and J. Psarras, "A multi-criteria approach for optimizing the placement of electric vehicle charging stations in highways," Energies, vol. 15, no. 24, p. 9445, 2022, doi: 10.3390/en15249445.

[36] M. H. Amini, M. P. Moghaddam, and O. Karabasoglu, "Simultaneous allocation of electric vehicles' parking lots and distributed renewable resources in smart power distribution networks," Sustainable Cities and Society, vol. 28, pp. 332–342, 2017, doi: 10.1016/j.scs.2016.10.006.

[37] T. Unterluggauer, J. Rich, P. B. Andersen, and S. Hashemi, "Electric vehicle charging infrastructure planning for integrated transportation and power distribution networks: A review," ETransportation, vol. 12, p. 100163, 2022, doi: 10.1016/j.etran.2022.100163.

[38] S. Kawambwa, R. Mwifunyi, D. Mnyanghwalo, N. Hamisi, E. Kalinga, and N. Mvungi, "An improved backward/forward sweep power flow method based on network tree depth for radial distribution systems," Journal of Electrical Systems and Information Technology, vol. 8, pp. 1–18, 2021, doi: 10.1186/s43067-021-00031-0.

[39] S. Ermiş, "Multi-objective optimal power flow using a modified weighted teaching-learning based optimization algorithm," Electric Power Components and Systems, vol. 51, no. 20, pp. 2536–2556, 2023, doi: 10.1080/15325008.2023.2239237.

[40] G. Wang, Z. Xu, F. Wen and K. P. Wong, "Traffic-Constrained Multiobjective Planning of Electric-Vehicle Charging Stations," in IEEE Transactions on Power Delivery, vol. 28, no. 4, pp. 2363-2372, Oct. 2013, doi: 10.1109/TPWRD.2013.226914.

[41] F. Zou, D. Chen, and J. Wang, "An improved teaching-learning-based optimization with the social character of PSO for global optimization," Computational Intelligence and Neuroscience, vol. 2016, no. 1, p. 4561507, 2016, doi: 10.1155/2016/4561507.

Divya Bharathi Raj (Member, IEEE) received a Bachelor's degree in Electrical and Electronics Engineering in 2018 and a Master's degree in Power Systems Engineering in 2021 from College of Engineering Guindy, Anna University and is currently working towards a doctorate in Electrical and Electronics Engineering at National Institute of Technology, Tiruchirappalli. Her area of research includes Optimization techniques, EV charging station planning, routing techniques and Distributed Generation units. The proposed work is the research project of this author.

Venkatakirthiga Murali (M'13–SM'19) received a B.E. degree in Electrical and Electronics from Bharathidasan University, Tiruchirappalli, India, in 2000, and M.Tech. degree in Power Systems and a Doctorate in Distributed Generation and Microgrids from the National Institute of Technology Tiruchirappalli (NITT), Tiruchirappalli, in 2004 and 2014, resp. She is currently working as a Professor with the Department of Electrical and Electronics Engineering, NITT. She has a total teaching experience of 19 years and serves as a reviewer to many reputed international journals. Her research interests include power systems, HVDC systems, distribution systems, and electrical machines. She is also a Fellow Institution of Engineers, India. This author serves as the research supervisor for the first author and for the proposed project work.